IEEE Photonics Journal
An IEEE Photonics Society Publication

Open Access

Photonic Generation of Microwave Frequency Shift Keying Signal Using a Polarization Maintaining FBG

Volume 10, Number 3, June 2018

Jia Ye
Lianshan Yan
Houjun Wang
Wei Pan
Bin Luo
Xihua Zou

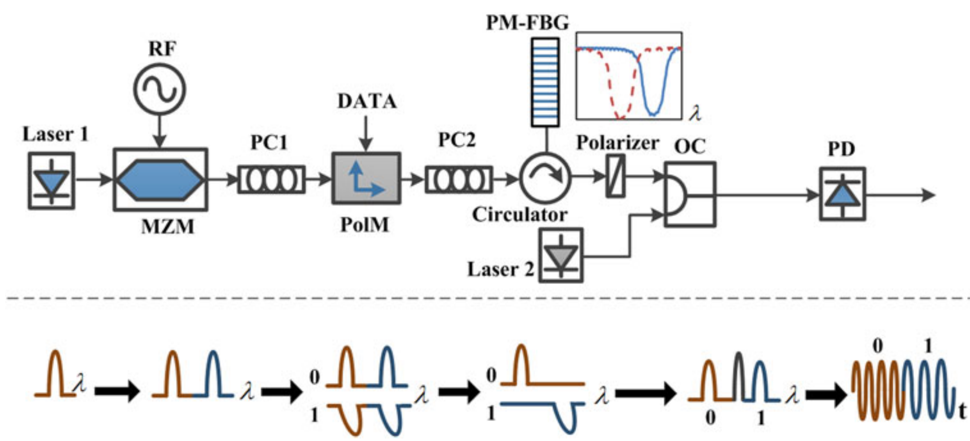

DOI: 10.1109/JPHOT.2017.2772778
1943-0655

Photonic Generation of Microwave Frequency Shift Keying Signal Using a Polarization Maintaining FBG

Jia Ye, Lianshan Yan, Houjun Wang, Wei Pan, Bin Luo, and Xihua Zou

Center for Information Photonics and Communications, School of Information Science and Technology, Southwest Jiaotong University, Chengdu 610031, China

DOI:10.1109/JPHOT.2017.2772778

Manuscript received October 15, 2017; revised November 7, 2017; accepted November 7, 2017. Date of publication November 13, 2017; date of current version May 18, 2018. This work was supported in part by the National High Technology Research and Development Program of China under 2015AA016903 and in part by the National Natural Science Foundation of China under Grants 61405165, 61775185, and 61335005. Corresponding author: Jia Ye (e-mail: jiaye@swjtu.edu.cn).

Abstract: A photonic generation of microwave frequency shift keying signal (FSK) with large frequency tunability is proposed and experimentally demonstrated. A polarization modulator combined with a polarization maintaining fiber Bragg grating is used to transform a carrier-suppressed double sideband signal to a wavelength-shift-keying one, which is subsequently mixed with a tunable optical source to achieve frequency modulation. A proof-of-concept experiment is demonstrated to obtain an FSK signal at 9.5/12.5 GHz. The carrier frequency has been tuned from 7.2 to 14.8 GHz by adjusting the laser wavelength. Moreover, a radio over fiber transmission link is established to investigate the transmission performance of the generated FSK signal. The bit-error-rate curve of the received FSK signal at 9.5/12.5 GHz for a 5-km single mode fiber and 2-m wireless transmission is presented.

Index Terms: Microwave signal generation, frequency shift keying, polarization maintaining fiber Bragg grating.

1. Introduction

As wireless access network advances toward higher capacity and quality to provide broadband and stable real-time services, there has been an increasing effort in exploiting the large unused bandwidths of sub-millimeter or millimeter-wave frequency regions [1]–[3]. This is a fundamental driver that has led to new technologies which can generate microwave signals with high frequency and specific modulation format. In addition, the generated microwave signals should be distributed to a remote site for many applications [4]–[5]. Thanks to the inherent large bandwidth and low-loss of optical fiber, photonic radiofrequency technology has emerged as one ideal solution to these problems.

Recently, many approaches for microwave signal generation have been proposed, which can be primarily categorized into two kinds. One is implemented by using spectral shaping and frequency to time mapping (FTTM) techniques [6]–[8]. Based on these techniques, microwave signals with particular envelop shape can be generated, which is widely used in radar system, sensor networks, and etc. The other kind is based on the frequency beating of two optical waves at a photodetector

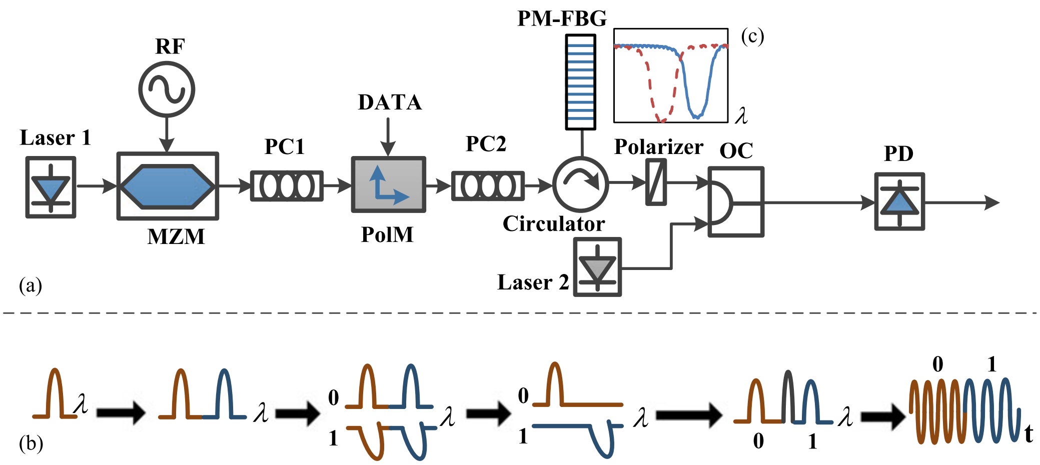

Fig. 1. Conceptual diagram of the proposed FSK signal generator, (a) setup diagram; (b) the illustration of the signal variation; (c) the response function of the PM-FBG.

[9]–[11]. It is usually employed in a radio over fiber system to obtain high-quality microwave signals with various modulation formats, including amplitude shift keying (ASK), phase shift keying (PSK) and high-order modulation format [12]–[13]. Besides the mentioned modulation formats, frequency shift keying is also an important one for wireless communication. Recently, a research reports that by using the FSK technique combined with other frequently-used modulation methods (i.e., phase modulation, quadrature amplitude modulation, etc.) the transmitted wireless signals exhibit better immunity to the inter-cell interference (ICI) induced channel impairments in a cellular wireless communication system, that is, the signal performance can be improved at the overlapped area under the coverage of multi-basestations by using FSK as an assistive modulation technique [14]. It is a significative finding while microcellular architecture with a large deployment of antenna base-stations (BSs) becomes the trend. Several photonic schemes for the FSK signal generation with high frequencies have been proposed [15]–[17]. In [16], a single-drive Mach-Zehnder modulator (MZM) is employed to generate FSK signals with particular carrier frequencies. In [17], microwave signals with different frequencies can be obtained by choosing different interference delays to generate two types of spectral shapes and map them into temporal domain by frequency to time mapping (FTTM).

In this paper, a novel photonic scheme for microwave FSK signal generation with large frequency tunability is proposed. A polarization modulator (PolM) combined with a polarization maintaining fiber Bragg grating is employed to modulate the output optical wavelength according to the baseband data stream. Then a FSK signal is generated through the optical heterodyning at a photodetector by mixing with an additional tunable optical source. Compared with the FTTM-based generation scheme, the proposed scheme can obtain a high-quality RF signal with large frequency tunability. In the proof-of-concept experiment, a FSK signal at 9.5/12.5 GHz is generated. By tuning the wavelength of the local laser, the carrier frequencies of the generated FSK signal are verified to be adjustable. Moreover, the proposed signal generation scheme has been demonstrated in a distributed RoF transmission system. A 1 Gbit/s FSK signal with the carrier frequencies of 9.5/12.5 GHz is generated and transmitted over a 5 km optical fiber and 2 m wireless transmission.

2. Principle and Theoretical Analysis

Fig. 1 shows the conceptual diagram of the proposed FSK signal generation, which is based on optical heterodyning. In the setup, a single-frequency light source from an optical continuous wave (CW) laser is sent to an Mach-Zehnder modulator (MZM), which is driven by a RF signal with the frequency Ω. The MZM is biased at null to achieve carrier suppressed double (CS-DSB) sideband modulation. Under the condition of small signal modulation, the output signal can be approximately described as

$$E_{out}(t) \approx E_0 J_1(\beta_1 \pi)\left[e^{j(\omega+\Omega)t} + e^{j(\omega-\Omega)t}\right] \tag{1}$$

where E_0 and ω are the amplitude and frequency of the input optical signal respectively. $J_1(\bullet)$ denotes the first order Bessel function. β_1 equals V_1/V_π where V_1 is the voltage of the RF signal and V_π is the half-wave voltage of the MZM.

Then the signal is poured into a polarization modulator (PolM). The PolM is a special phase modulator that can support both TE and TM modes with opposite phase modulation indices [18]. When the incident light is oriented at an angle of 45° to one principal axis of the PolM by using a polarization controller (PC), complementary phase modulation signals are generated along the two principal axes. Consequently, the output of the PolM along the two polarization axes can be expressed as

$$\begin{bmatrix} E_x \\ E_y \end{bmatrix} = \begin{bmatrix} E_0 J_1(\beta_1\pi)\left[e^{j(\omega+\Omega)t+j(A_i\beta_2\pi)} + e^{j(\omega-\Omega)t+j(A_i\beta_2\pi)}\right] \\ E_0 J_1(\beta_1\pi)\left[e^{j(\omega+\Omega)t-j(A_i\beta_2\pi)} + e^{j(\omega-\Omega)t-j(A_i\beta_2\pi)}\right] \end{bmatrix} \tag{2}$$

where $\beta_2 = V_2/V'_\pi$ is the modulation index of the PolM. V_2 is the voltage of the baseband signal. V'_π is the the half-wave voltage of the PolM. A_i is the binary data. Generally, the voltage of the baseband signal is tuned to make β_2 equal 1/2 to achieve polarization modulation.

When the output signals are sent to a PM-FBG with its principal axis oriented at an angle of 45° to one principal axis of the PolM, we obtain

$$\begin{bmatrix} E'_x \\ E'_y \end{bmatrix} = \begin{bmatrix} \frac{\sqrt{2}}{2}(E_x + E_y) \\ \frac{\sqrt{2}}{2}(E_x - E_y) \end{bmatrix} = \begin{bmatrix} E_0 J_1(\beta_1\pi)\cos\left(\frac{\pi}{2}A_i\right)\left[e^{j(\omega+\Omega)t} + e^{j(\omega-\Omega)t}\right] \\ E_0 J_1(\beta_1\pi)\, j\sin\left(\frac{\pi}{2}A_i\right)\left[e^{j(\omega+\Omega)t} + e^{j(\omega-\Omega)t}\right] \end{bmatrix} \tag{3}$$

It can be seen from the (3), the binary data A_i determines the polarization of the output signal.

As shown in Fig. 1(c), the response function of the PM-FBG depends on the polarization state of the input signal [19]. The wavelengths of the two signal sidebands are adjusted to locate at the two notches of the PM-FBG, respectively. Under ideal condition, the reflected signal of the PM-FBG can be expressed as

$$\begin{bmatrix} E'_x \\ E'_y \end{bmatrix} = \begin{bmatrix} \frac{\sqrt{2}}{2}(E_x + E_y) \\ \frac{\sqrt{2}}{2}(E_x - E_y) \end{bmatrix} = \begin{bmatrix} E_0 J_1(\beta_1\pi)\cos\left(\frac{\pi}{2}A_i\right)\left[e^{j(\omega+\Omega)t}\right] \\ E_0 J_1(\beta_1\pi)\, j\sin\left(\frac{\pi}{2}A_i\right)\left[e^{j(\omega-\Omega)t}\right] \end{bmatrix} \tag{4}$$

Through a polarizer with an angle of 45° to the incident signal polarization, the two polarization components of the signal are aligned at the same direction. Then the signal can be described as

$$\begin{aligned} E'_{out}(t) &= \frac{\sqrt{2}}{2} E_0 J_1(\beta_1\pi)\left[\cos\left(\frac{\pi}{2}A_i\right)e^{j(\omega+\Omega)t} + j\sin\left(\frac{\pi}{2}A_i\right)e^{j(\omega-\Omega)t}\right] \\ &= \begin{cases} \frac{\sqrt{2}}{2} E_0 J_1(\beta_1\pi) \bullet e^{j(\omega+\Omega)t}, A_i = 0 \\ \frac{\sqrt{2}}{2} E_0 J_1(\beta_1\pi) \bullet j e^{j(\omega-\Omega)t}, A_i = 1 \end{cases} \end{aligned} \tag{5}$$

It can be seen that the obtained signal is wavelength modulated. After the frequency beating with another CW light at the photodetector, the output photocurrent can be given by

$$I_{out}(t) = \begin{cases} 2\sqrt{P_1 P_2}\cos\left[(\omega + \Omega - \omega_1)t + \Delta\phi\right], A_i = 0 \\ 2\sqrt{P_1 P_2}\cos\left[(\omega_1 + \Omega - \omega)t + \Delta\phi\right], A_i = 1 \end{cases} \tag{6}$$

where P_1 is the power of E'_{out}, P_2 and ω_1 is the power and frequency of the CW source respectively, $\Delta\phi$ is the phase difference [3]. In (6), the direct current has already been omitted. It can be found

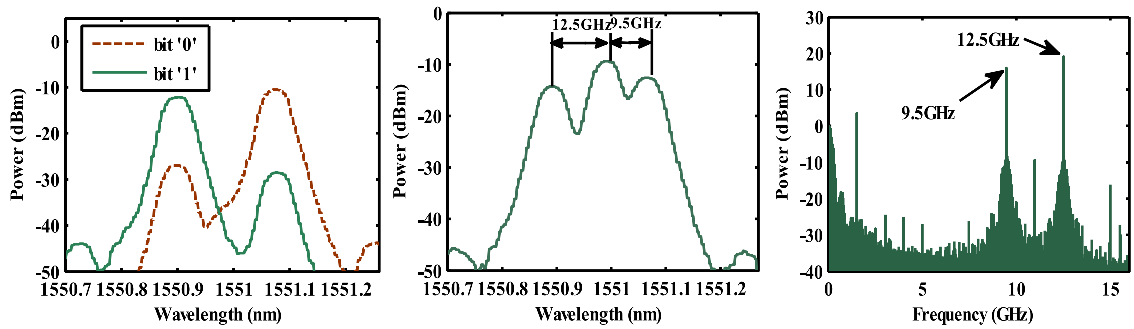

Fig. 2. (a) The output spectra from the PM-FBG for bit '0' and bit '1', (b) the optical spectrum coupled with the CW source of Laser2 for the PRBS data stream, (c) the electrical spectrum of the generated FSK signal.

that the generated RF signal is a FSK signal with the frequencies as

$$\begin{cases} f_1 = [\Omega + (\omega - \omega_1)] \\ f_2 = [\Omega - (\omega - \omega_1)] \end{cases}, \ \omega - \Omega < \omega_1 < \omega + \Omega \tag{7}$$

Consequently, the frequencies of the generated FSK signal can be continuously tuned by adjusting the RF signal frequency Ω and the wavelength difference between the two CW laser sources in the generator.

3. Experiments

3.1 FSK Signal Generation and Its Tunability

Firstly, the proposed photonic scheme for the generation of a FSK signal is experimentally demonstrated. The experimental setup is shown in Fig. 1(a). A tunable CW laser (Agilent 8163A, with linewidth ~60 MHz) is modulated by a MZM, which is driven by a RF signal with the frequency of 11 GHz. The MZM is biased at null to achieve CS-DSB modulation to generate a two-tone signal with the frequency spacing of 22 GHz. A PC is placed subsequently to orient the incident polarization at an angle of 45° to one principal axis of the PolM. Then the polarization modulated signal is sent into the PM-FBG with the response function as shown in Fig. 1(c). One frequency component of the two-tone signal is filtered out for each polarization, i.e., a wavelength shift keying signal is reflected by the PM-FBG and poured into one port of a 3dB optical coupler (OC) via the circulator.

In order to verify the feasibility of the wavelength shift keying procedure, the two individual optical spectra for bit '0' and bit '1' have been obtained while the data streams applied on the PolM are initialized to all zeros and all ones respectively. The wavelength of the Laser1 is set as 1550.98 nm. The output spectra from the PM-FBG for bit '0' and bit '1' are shown in Fig. 2(a). It can be seen that the wavelengths of the two sidebands are respectively 1550.89 nm and 1551.07 nm with a frequency spacing of 22 GHz. Then the optical spectrum of the received signals coupling with the LO source is present in Fig. 2.(b). Then the baseband data applied on the PolM is set to be a 0.5 Gbit/s PRBS stream. After being coupled with the local CW source with the wavelength of 1550.99 nm, the output spectrum is shown in Fig. 2(b). The frequency differences between the local source and the two sidebands of the transmitted CS-DSB signal are 12.5 GHz and 9.5 GHz, respectively.

After frequency beating at a PD, a FSK signal can be obtained. The electrical spectrum of the generated signal is shown in Fig. 2(c). There are two carrier frequencies at 9.5 Gz and 12.5 GHz, which are the dominant parts in the spectrum. Besides, the 1.3 GHz frequency component is generated from the frequency beating of the two CW sources, which can be filtered out easily as it is far from the two carrier frequencies. Then the temporal waveform of the generated signal is

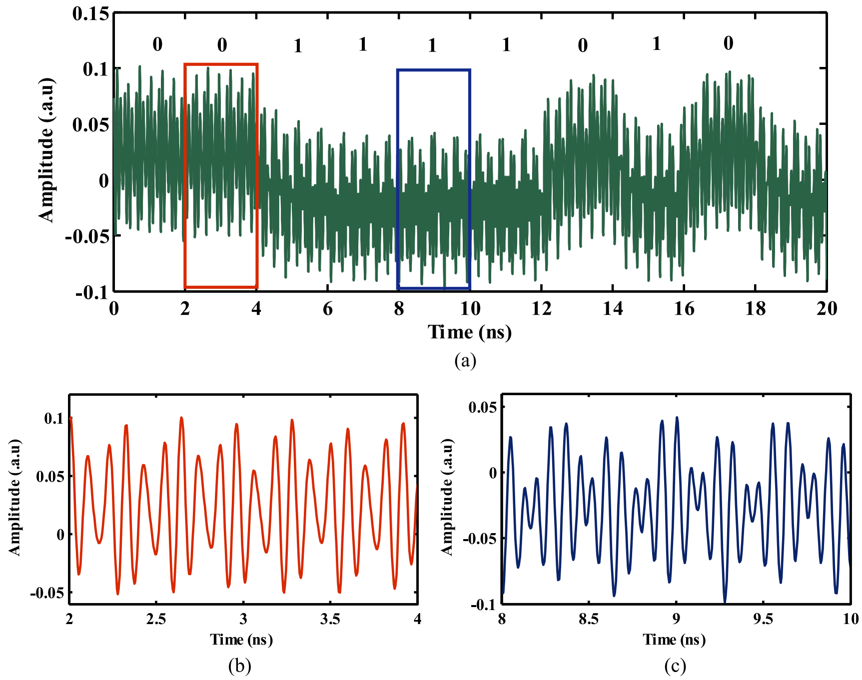

Fig. 3. (a) The waveform of the generated FSK signal in the duration of 20 ns. (b) the enlarged view of the waveform during 2 ns∼4 ns at 9.5 GHz; (c) the enlarged view of the waveform during 8 ns∼10 ns at 12.5 GHz.

captured by a real-time oscilloscope (Lecroy WaveMaster 813i). Fig. 3(a) displays the waveform in the duration of 20 ns. The 9.5 GHz and 12.5 GHz RF signal are marked as bit '0' and bit '1' respectively at the top of the figure. There is an amplitude difference between the 9.5 GHz RF signal and the 12.5 GHz RF signal, which is due to the different reflectivity of the PM-FBG. In order to clearly compare the signals at the two carrier frequencies, enlarged views of the waveform in the red and blue rectangle are shown in Fig. 3(b) and (c). As the data rate is 0.5 Gbit/s, i.e., the symbol period is 2 ns, Fig. 3(b) and (c) show the waveform in one symbol period, corresponding to the carrier frequencies of 9.5 GHz and 12.5 GHz, respectively. It can be seen from the figure that there is a periodic amplitude fluctuation of the waveform, which is mainly because only 3 or 4 samples are captured in one period of the two carrier frequencies as the sampling rate is 40 GS/s. When the carrier frequency is not an integral multiple of the sampling rate, the obtained waveform curve will exhibit a period fluctuation.

In order to investigate the tunability of the proposed FSK signal generation approach, the wavelength of the local CW source is tuned to adjust the carrier frequencies. The obtained signal frequency as a function of the laser wavelength is shown in Fig. 4. The red square and green circle curve represent the two carrier frequencies respectively. It can be seen that the two carrier frequencies are approximately changed linearly with the optical wavelength, which matches well with the (7). It is verified that the carrier frequency is continuously tunable in the range of 7.2∼14.8 GHz. Actually, the tunable range is just limited by the bandwidth of the PD. Due to the (7), arbitrary carrier frequencies can be achieved by properly setting the RF signal frequency and the wavelength difference between the two CW laser sources. The insets Fig. 4(a) and (b) display the waveform of the generated frequency at 13.4 GHz and 9.85 GHz, respectively.

3.2 Transmission Demonstration in a RoF Link

A RoF transmission system is established to investigate the transmission performance of the generated tunable FSK signal, as shown in Fig. 5. The experimental system is constructed to

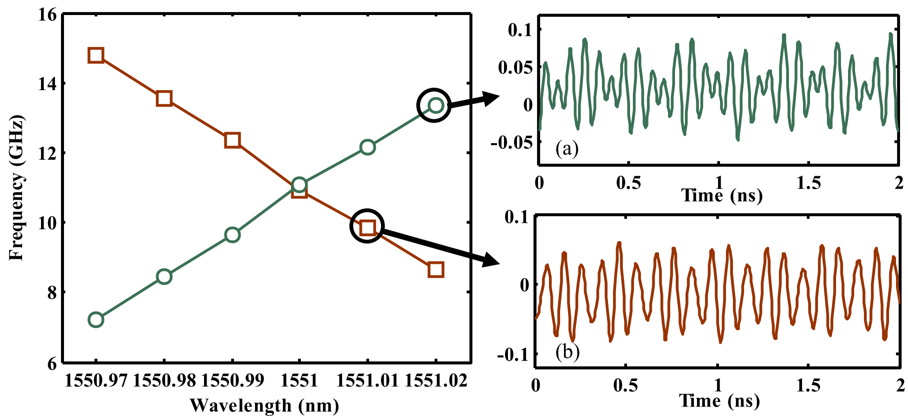

Fig. 4. The generated carrier frequencies versus the wavelength of the local CW source, the waveform at (a) 13.4 GHz and (b) 9.85 GHz.

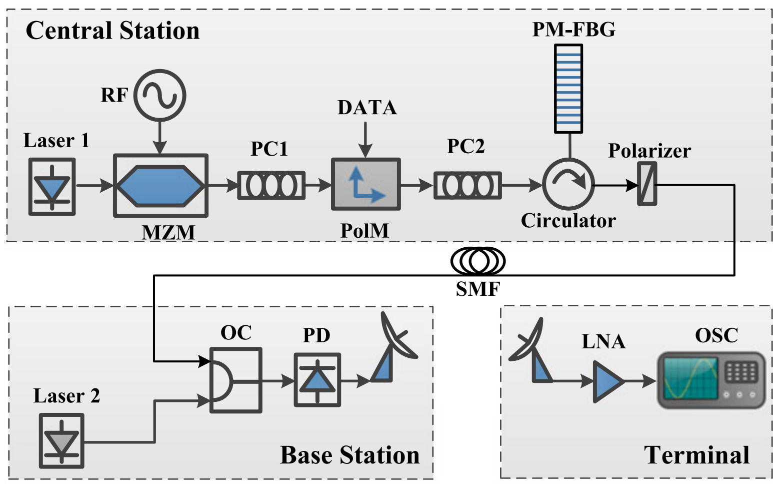

Fig. 5. Experimental setup of the RoF transmission system.

simulate the transmission among a central station (CS), a base station (BS) and a wireless terminal. The FSK signal generator is distributed at the CS and BS, which is corresponding to a RoF link based on the optical heterodyning technique. At the CS, a 1550.98 nm CW laser followed by a MZM driven by a RF signal at 11 GHz is employed to produce a CS-DSB signal. The wavelengths of the two sidebands are 1550.89 nm and 1551.07 nm, respectively. A PolM driven by a 1 Gbit/s PRBS data stream and a PM-FBG are grouped to achieve wavelength shift keying. A polarizer is employed subsequently to align the wavelength-modulated signal at the same polarization. Then the generated signal is launched into a 5 km single mode fiber (SMF). At the BS, a local laser is used to provide a CW source at 1550.99 nm. The received DSB signal is coupled with the local source and sent to a PD (HP 11982A) to achieve frequency beating. A FSK signal with the carrier frequencies of 9.5/12.5 GHz is obtained and transmitted by a directional antenna with the bandwidth of 8∼14 GHz. Finally, the FSK wireless signal is received by the same type antenna and amplified with a low noise amplifier (LNA). A real-time oscilloscope (14 GHz bandwidth and 40 GS/s sampling rate) is used to capture the FSK signal.

Fig. 6(a) displays the spectrum of the received RF signal. Offline digital signal processing is implemented to demodulate the FSK signal. Firstly, the received signal is mixed with two RF carriers at 12.5 GHz and 9.5 GHz respectively and poured into low-pass filters to filter out the undesired frequency components. Two baseband on-off keying (OOK) signal streams with opposite

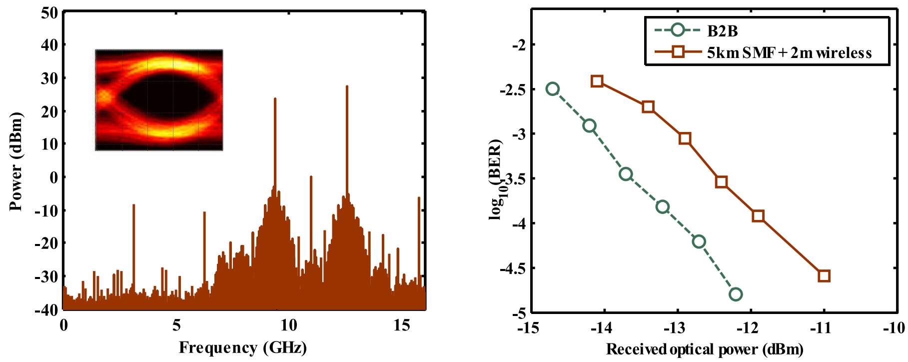

Fig. 6. (a) Spectrum of the received signal and eyediagram after demodulation; (b) BER versus the received optical power for B2B and optical wireless transmission.

polarity are obtained corresponding to the 12.5 GHz and 9.5 GHz, respectively. Then a balanced differential processing is implemented to convert the two single-ended signals to a balanced signal. The eyediagram of the obtained OOK signal is shown in the inset of Fig. 6(a). Finally, the bit error rate (BER) curve is measured and shown in Fig. 6(b). The green dashed line denotes the BER curve for the back to back case and the red solid line is the BER curve for the 5 km SMF and 2 m wireless transmission. It can be seen that −13.9 dBm incident optical power is needed to reach the BER of 10^{-3} for the back to back case. Under the fiber and wireless transmission scenario, one more decibel incident power is required.

4. Conclusion

In this paper, a photonic approach for microwave FSK signal generation with large frequency tunability has been proposed and experimentally demonstrated. Firstly, the waveforms of the FSK signals with various carrier frequencies have been presented. The experiment results show that the carrier frequency can be continuously tuned by adjusting the wavelength of the local laser. Then the performance of the obtained FSK signals has been investigated in a RoF transmission link based on optical heterodyning. Offline DSP has been implemented to demodulate the received signals and the BER curves for the back to back and 5 km SMF +2 m wireless transmission have been measured, which has verified the feasibility of the proposed scheme in a RoF transmission system.

Acknowledgment

The authors wish to thank the anonymous reviewers for their valuable suggestions.

References

[1] A. J. Seeds and K. J. Williams, "Microwave photonics," *J. Lightw. Technol.*, vol. 24, no. 3, pp. 4628–4641, Dec. 2006.
[2] J. Capmany and D. Novak, "Microwave photonics combines two worlds," *Nature Photon.*, vol. 1, pp. 319–330, 2007.
[3] J. P. Yao, "Microwave photonics," *J. Lightw. Technol.*, vol. 27, pp. 314–335, Feb. 2009.
[4] C. Lim *et al.*, "Fiber-wireless networks and subsystem technologies," *J. Lightw. Technol.*, vol. 28, no. 4, pp. 390–405, Feb. 2010.
[5] C. Yin *et al.*, "Microwave photonic frequency up-convertor with frequency doubling and compensation of chromatic-dispersion-induced power fading," *IEEE Photon. J.*, vol. 9, no. 3, 2017, Art. no. 5502307.
[6] J. Chou, Y. Han, and B. Jalali, "Adaptive RF-photonic arbitrary waveform generator," *IEEE Photon. Technol. Lett.*, vol. 15, no. 4, pp. 581–583, Apr. 2003.
[7] Y. Dai, J. Li, Z. Zhang, F. Yin, W. Li, and K. Xu, "Real-time frequency-to-time mapping based on spectrally-discrete chromatic dispersion," *Opt. Exp.*, vol. 25, no. 14, 2017, Art. no. 16660.
[8] J. Ye *et al.*, "Photonic generation of triangular-shaped pulses based on frequency to time conversion," *Opt. Lett.*, vol. 36, no. 8, pp. 1458–1460, 2011.

[9] C. Lin, J. Chen, S. Dai, P. Peng, and S. Chi, “Impact of nonlinear transfer function and imperfect splitting ratio of MZM on optical up-conversion employing double sideband with carrier suppression modulation,” *J. Lightw. Technol.*, vol. 26, no. 15, pp. 2449–2459, Aug. 2008.

[10] Y. G. Shee *et al.*, “All-optical generation of a 21 GHz microwave carrier by incorporating a double-Brillouin frequency shifter,” *Opt. Lett.*, vol. 35, no. 9, pp. 1461–1463, 2010.

[11] J. Yu, Z. Jia, and L. Yi, “Optical millimeter-wave generation or up-conversion using external modulators,” *IEEE Photon. Technol. Lett.*, vol. 18, no. 1, pp. 265–267, Jan. 2006.

[12] W. Li, W. T. Wang, W. H. Sun, L. X. Wang, and N. H. Zhu, “Photonic generation of arbitrarily phase-modulated microwave signals based on a single DDMZM,” *Opt. Exp.*, vol. 22, no. 7, pp. 7446–7457, 2014.

[13] J. Ye *et al.*, “Two-dimensionally tunable microwave signal generation based on optical frequency-to-time conversion,” *Opt. Lett.*, vol. 35, no. 15, pp. 2606–2608, 2010.

[14] S. Hong, S. Min, C. Lim, K. Cheun, and S. Cho, “FQAM: A modulation scheme for beyond 4G cellular wireless communication systems,” in *Proc. IEEE Globecom Workshop*, 2013, pp. 25–30

[15] L. Huang *et al.*, “Photonic generation of microwave frequency shift keying signals,” *IEEE Photon. Technol. Lett.*, vol. 28, no. 18, pp. 1928–1931, Sep. 2016.

[16] P. Cao, X. Hu, L. Zhang, J. Wu, X. Jiang, and Y. Su, “Photonic generation of microwave frequency shift keying signal using a single-drive Mach–Zehnder modulator,” *Opt. Exp.*, vol. 22, no. 12, pp. 14433–14440, 2014.

[17] H. Mu, H. Xia, and J. Yao, “A frequency shift keying transmitter based on incoherent frequency-to-time mapping for free-space optical communications,” *Microw. Photon.*, 2010, pp. 208–211.

[18] X. Zou and J. Yao, “Repetition-rate-tunable return-to-zero and carrier-suppressed return-to-zero optical pulse train generation using a polarization modulator,” *Opt. Lett.*, vol. 34, no. 3, pp. 313–315, 2009.

[19] X. Feng, Z. Li, B. Guan, C. Lu, H. Y. Tam, and P. K. A. Wai, “Switchable UWB pulse generation using a polarization maintaining fiber Bragg grating as frequency discriminator,” *Opt. Exp.*, vol. 18, no. 4, pp. 3643–3648, 2010.

[20] A. J. Seeds, “Microwave photonics,” *IEEE Trans. Microw. Theory Techn.*, vol. 50, no. 3, pp. 877–887, Mar. 2002.